EFDA–JET–CP(12)05/02

Ph. Mertens, J.W. Coenen, S. Devaux, S. Jachmich, I. Balboa, G.F. Matthews,
V. Riccardo, B. Sieglin, V. Tanchuk, A. Terra, V. Thompson, U. Samm
and JET EFDA contributors

Power Handling of the Bulk Tungsten Divertor Row at JET: First Measurements and Comparison to the GTM Thermal Model

Power Handling of the Bulk Tungsten Divertor Row at JET: First Measurements and Comparison to the GTM Thermal Model

Ph. Mertens[1], J.W. Coenen[1], S. Devaux[2], S. Jachmich[3], I. Balboa[4], G.F. Matthews[4],
V. Riccardo[4], B. Sieglin[2], V. Tanchuk[5], A. Terra[1], V. Thompson[4], U. Samm[1]
and JET EFDA contributors*

JET-EFDA, Culham Science Centre, OX14 3DB, Abingdon, UK

[1]Institute of Energy and Climate Research IEK-4 (Plasma Physics), Forschungszentrum Jülich GmbH,
Association EURATOM-FZJ, D-52425 Jülich, Germany
[2]Max-Planck-Institut für Plasmaphysik, EURATOM Association, D-85748 Garching, Germany
[3]Laboratory for Plasma Physics-ERM/KMS, Association EURATOM-Belgian State, B-1000 Brussels, Belgium
[4]EURATOM-CCFE Fusion Association, Culham Science Centre, OX14 3DB, Abingdon, OXON, UK
[5]SINTEZ Scientific Technical Centre, D.V. Efremov SRIEA, RUS-196641, St Petersburg, Russia
** See annex of F. Romanelli et al, "Overview of JET Results",*
(23rd IAEA Fusion Energy Conference, Daejon, Republic of Korea (2010)).

Preprint of Paper to be submitted for publication in Proceedings of the
27th Symposium on Fusion Technology (SOFT), Liege, Belgium
24th September 2012 - 28th September 2012

ABSTRACT

The design of the tile assemblies of the bulk tungsten divertor row in JET was improved in the course of several experiments as far as the power and energy performances are concerned: many prototypes were exposed to high heat fluxes in several electron and ion beam facilities during the development phase. These experiments were carried out in parallel with extensive modelling of the complete tungsten tile assembly in the so-called Global Thermal Model (GTM). The goal was to understand the heat flow from the plasma-facing surface through the supporting structure down to the base plate of the JET MkII divertor sufficiently to be able to later interpret operational data from the torus. Temperatures measured in the torus are in good agreement (–10/+15%) with the model. Some characteristic times show stronger deviations, with no incidence on the highest temperature at all times.

1. INTRODUCTION

The bulk tungsten divertor tiles of the ITER-like Wall at JET are unique in the sense that they face high loads (up to $9MW/m^2$ for a total energy density of $60\,MJ/m^2$ maximum over the pulse length) without active cooling. Their design [1] was primarily driven by very restrictive constraints with respect to the electromagnetic forces, to existing fixings in the base plate, to the requirement of perfect shadowing of all front edges and to the decision of subjecting the tungsten to pure compression due to its brittleness at low temperatures and a possible loss of ductility [2]. As far as the power and energy performance are concerned, prototype tile assemblies were mainly designed ‘by experiment’: several protoypes were exposed to high heat fluxes in different electron and ion beam facilities during the development phase [3-5] and the results of an exposure in this sequence over several facilities, JUDITH-1, TEXTOR, JUDITH-2 were exploited to improve the detailed design for the next in a converging manner. The last two campaigns, in MARION, dealt with one stack of 24 tungsten lamellae in the frozen design which corresponded to the later assemblies (384 stacks) in the bulk tungsten divertor row.

These experiments were carried out in parallel with extensive modelling of the complete tungsten tile assembly within the so-called Global Thermal Model (GTM) [6]. The goal was to understand the heat flow from the plasma-facing surface through the supporting structure down to the base plate of the JET MkII structure sufficiently to be able to later interpret operational data from the actual torus. The thermocouple (TC) and infrared (IR) data in JET are of major importance for machine operation as they give indications on the permitted load range for the next plasma pulse.

2. EXPERIMENTAL

The 48 bulk tungsten tile assemblies which cover the full circumference of the bulk tungsten row consist of two sets of four stacks with 24 lamellae each (Fig.1). The stacks are aligned with the toroidal direction. The critical positions for temperature measurements were determined in the course of the experiments on various facilities described in the introduction.

The locations with highest priorities correspond to the setup which was chosen for the last exposures under the ion beam of MARION [4] and is shown in the left part of Fig. 2 (a).The tungsten temperature is measured with pyrometers and infrared cameras at the top, plasma-facing surface and with spring loaded thermocouples against the bottom of the tungsten tile. Other thermocouples record the temperature of the wedge carrier (Inconel 625) and of the clamping arrangement between the pack of insulating shims in the upper part and the actual flextures, spring discs in the lower pile. The 1-to-1 arrangement for JET is shown in Fig.2 (b), on the right side. As the access, that is the number of available wired sockets is limited, only three tile pairs are equipped with such TCs, which still provides some redundancy except for the temperature of the springs where only one thermocouple remains in operation. In these assemblies, all stacks except stack A (the inner one, i.e. to the high field side) can be monitored with respect to the temperature of the underside of the tungsten tile and of the wedge carrier.

3. RESULTS AND DISCUSSION

The very first experiment was intended to verify the shadowing properties. It turned out that the installed tile geometry is close to nominal. The largest vertical deviations ($\Delta z \leq 140$mm) were revealed in the survey which was performed just after installation. The first plasmas to check the shadowing properties (JPN 80751-56 where JPN stands for JET Pulse Number) confirmed the limited deviations and showed, with a scan of the magnetic field strength, that safe operation can take place down to roughly $q_{95} \geq 2.45$. Tolerancing and inspection methods –Coordinate Measurement Methods (CMM) for quality assessment and laser Gap Gun *in situ*– proved effective. In this first series of pulses, the measured temperatures of the tungsten lamellae, at the bottom of the tungsten tile after equilibration, were in fair agreement with the model although the deposited energy was too low for a sound comparison with the thermal model (high error margin on very low temperatures): a measured temperature rise of $DT \sim 130$°C for 7.5 MJ/stack-row in a 5 s plateau versus $\Delta T \sim 400$°C for 20 MJ/stack-row in a 10 s pulse in the model; the agreement was assessed in terms of the ratio of the thermal impact factors

$$\frac{q_0}{A}\sqrt{t} = \frac{T}{2}\sqrt{\pi k \rho C}$$

where q_0 represents the incident heat flux, A the exposed area, k the heat conductivity of tungsten, ρ the density and C the heat capacity (from a 1D *Fourier* equation) as usual.

DISCUSSION OF TEMPERATURES

With increasing neutral beam power available, 3 pulses were analysed in more detail: 81510-511 (stacks C and D –Fig. 2b– at 5MW NBI) and 82394 (stack D with 12MW NBI). In those and similar cases, the temperatures match the model values within the following deviations

- surface of the tungsten tile: +/– 20% for temperatures in the range 500-800°C with a maximal deviation in the order of 100°C (the IR measurement tends to identify hot spots and is higher);
- the temperatures of the clamping springs are very close to the modelled temperatures

(±10°C) provided an offset of maximum 30°C is added to the recorded values. Note that the model was scrutinised and the equivalent thermal conductivities of contacts were adjusted with great care to converge to experimental values during the tests of all prototypes to account for the vulnerability of the flextures and the uncertainties in the models for thermal contacts [7-9]. This may partly explain the narrower deviations;

- wedge carrier wings: +10/+65°C in the range 150–300°C (the predicted temperatures are higher).

DISCUSSION OF CHARACTERISTIC TIMES AND ASSOCIATED TIME EVOLUTION OF THE CURVES.

The modelled time evolution of the temperatures at critical locations in the clamping and on the wedge carrier is shown in Fig. 3 below. Measured curves are shown for comparison.

The characteristic times, for instance the time to maximum or the time to 1/e decay display the following behaviour:

- the characteristic time for the measured temperature at the clamping springs, one of the most vulnerable components in the supporting structure, amounts to 850s, to be compared to the modelled 800 s. Taking into account the uncertainty on the exact distribution of the load on the upper surface of the tile, which may significantly affect the distribution between different clamping bolts and, accordingly, between sets of spring discs, this agreement is excellent (upper Fig.3);
- the temperature of the underside of the wedge rises to the maximum value in about 700 s which is much slower than the expected order of magnitude of 200s (lower Fig.3). This may be due to the actual location of the TC with respect to the selected nodes in the model and to fairly different resistances of thermal contacts along the way between model and experiment.

The reason for a good agreement in the time evolution in the first case and for the poorer match in the second one may be related to the fact that the first temperature (springs) corresponds to a high temperature path, even though it is 'slowed down' by the insulating shims, and the second temperature (carrier) is at the end of a low temperature path. Still, the inertial cooling tends to be a slow process anyway owing to the overall heat capacity of the assemblies (the only way to dump the gigantic heat wave) and to the limited contact – through Inconel legs - to the base plate of the divertor.

CONCLUSIONS

The results of the first experimental campaigns are in good agreement with the expected tungsten temperature rise on the surface: $DT_{W,surf} \leq 1000$°C with NBI heating powers up to 15MW for several seconds. A neutral beam power of 12MW for 5s, for instance, leads to a temperature rise of the surface of about 700°C. The average temperature of the bulk tungsten after the pulse agrees within ±15% with the modelled temperature range. Deviations of the carrier temperatures reach +10/+65°C with the supporting structure up to $T_{carrier} \leq 500$°C close to the end of the first campaign. Some of the characteristic times, from ~10s to 800s depending on the component considered, differ appreciably from the values expected from the model. This is not a concern, though, since all temperature curves merge below the envelope constituted by the highest one, which corresponds to the expected order of magnitude for the cooling. The tile is designed for a maximum local temperature of the plasma-facing tungsten of 2200°C and a maximal energy deposition of 60 MJ/m^2 (+0/-10%). The experimental behaviour of the row of bulk tungsten tiles during plasma operation is close to design values in a wide range of operational parameters with deposited energy densities around and slightly above 30 MJ/m^2 which corresponds to the pulses that could be analysed in the present frame.

ACKNOWLEDGEMENTS

The authors are thankful for the strong support of the JUDITH, TEXTOR and MARION teams in Jülich and, of course, of the JET Engineering team in Culham. This work, supported by the European Communities under the contract of Association between EURATOM and Forschungszentrum Jülich, was carried out within the framework of the European Fusion Development Agreement (EFDA). The views and opinions expressed herein do not necessarily reflect those of the European Commission.

REFERENCES

[1]. G.F. Matthews et al., Physica Scripta **T145** (2011), 014001 (6pp)
[2]. Ph. Mertens et al., Physica Scripta **T138** (2009), 014032 (5pp)
[3]. T. Hirai et al., Physica Scripta **T128** (2007) 144–149
[4]. Ph. Mertens et al., Fusion Engineering and Design **86** (2011) 1801–1804
[5]. Ph. Mertens et al., Journal of Nuclear Materials **415** (2011) S943–S947
[6]. S. Grigoriev et al., Fusion Engineering and Design **84** (2009) 853–858
[7]. L. Fletcher, P. Smuda, D. Gyorog, AIAA Journal 7/7 (1969) 1302–1309 –American Institute of Aeronautics and Astronautics, and corresponding NASA reports
[8]. M. Bahrami, J.R. Culham, M.M. Yovanovich, G.E. Schneider, Proc. HTC'03, ASME Summer Heat Transfer Conference (2003) ref. HT2003-47051, 21 pp.
[9]. M. Bahrami, J.R. Culham, M.M. Yovanovich, G.E. Schneider, Applied Mechanics Reviews **59**/1 (2006) 1–12.

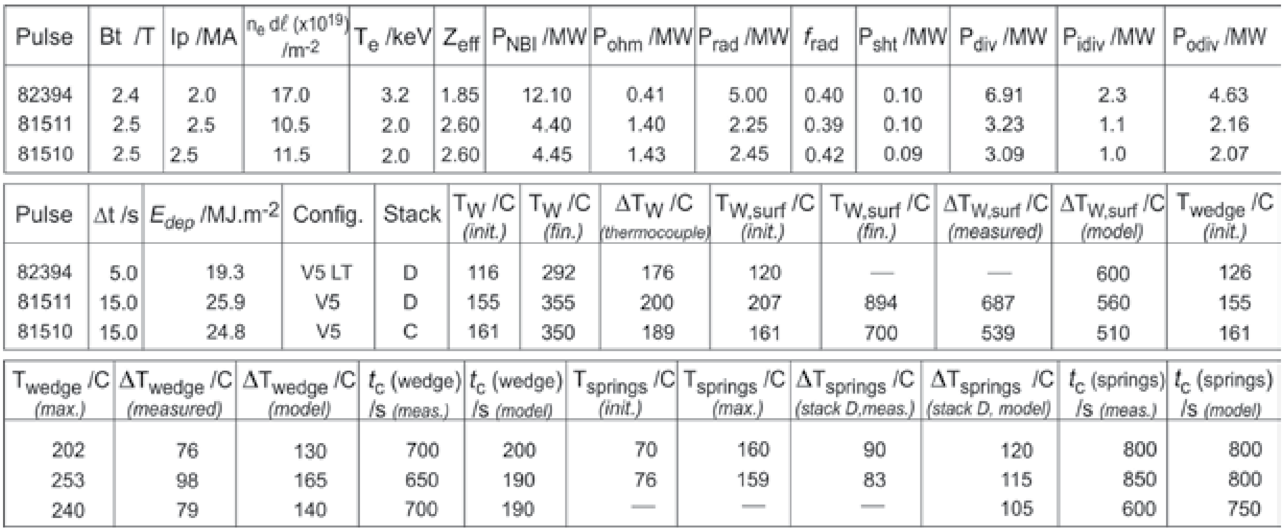

Pulse	Bt /T	Ip /MA	$n_e\,d\ell$ (x10^{19}) /m^{-2}	T_e /keV	Z_{eff}	P_{NBI} /MW	P_{ohm} /MW	P_{rad} /MW	f_{rad}	P_{sht} /MW	P_{div} /MW	P_{idiv} /MW	P_{odiv} /MW
82394	2.4	2.0	17.0	3.2	1.85	12.10	0.41	5.00	0.40	0.10	6.91	2.3	4.63
81511	2.5	2.5	10.5	2.0	2.60	4.40	1.40	2.25	0.39	0.10	3.23	1.1	2.16
81510	2.5	2.5	11.5	2.0	2.60	4.45	1.43	2.45	0.42	0.09	3.09	1.0	2.07

Pulse	Δt /s	E_{dep} /MJ.m^{-2}	Config.	Stack	T_W /C *(init.)*	T_W /C *(fin.)*	ΔT_W /C *(thermocouple)*	$T_{W,surf}$ /C *(init.)*	$T_{W,surf}$ /C *(fin.)*	$\Delta T_{W,surf}$ /C *(measured)*	$\Delta T_{W,surf}$ /C *(model)*	T_{wedge} /C *(init.)*
82394	5.0	19.3	V5 LT	D	116	292	176	120	—	—	600	126
81511	15.0	25.9	V5	D	155	355	200	207	894	687	560	155
81510	15.0	24.8	V5	C	161	350	189	161	700	539	510	161

T_{wedge} /C *(max.)*	ΔT_{wedge} /C *(measured)*	ΔT_{wedge} /C *(model)*	t_c (wedge) /s *(meas.)*	t_c (wedge) /s *(model)*	$T_{springs}$ /C *(init.)*	$T_{springs}$ /C *(max.)*	$\Delta T_{springs}$ /C *(stack D,meas.)*	$\Delta T_{springs}$ /C *(stack D, model)*	t_c (springs) /s *(meas.)*	t_c (springs) /s *(model)*
202	76	130	700	200	70	160	90	120	800	800
253	98	165	650	190	76	159	83	115	850	800
240	79	140	700	190	—	—	—	105	600	750

Table 1: Plasma parameters and temperatures for the pulses discussed in the text.

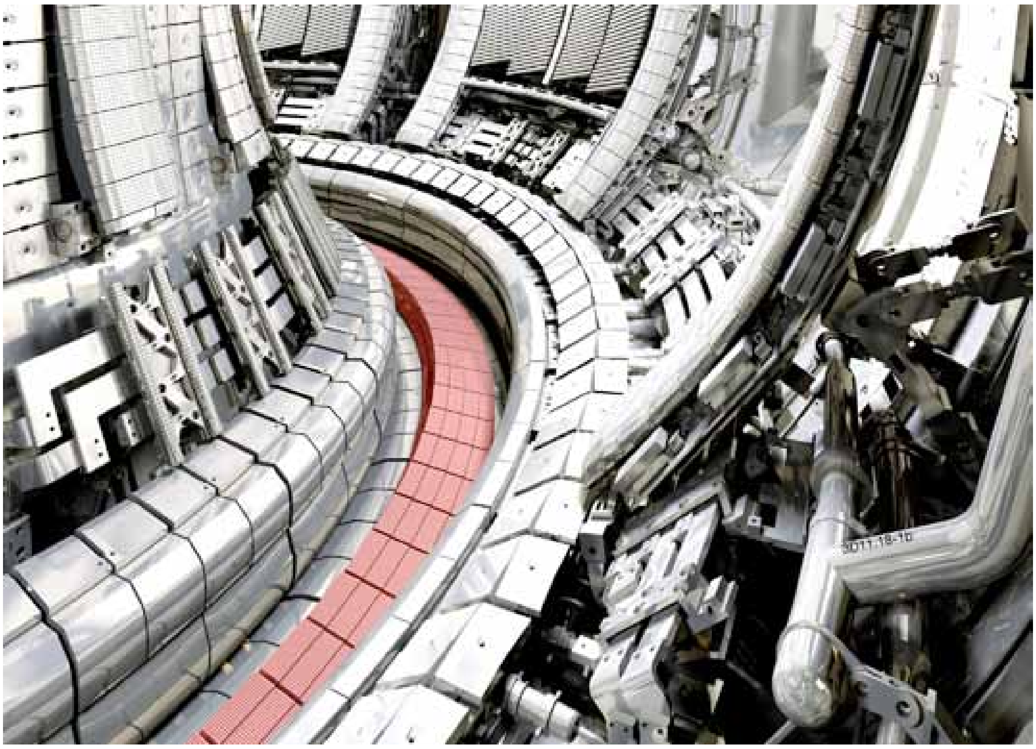

Figure 1: The bulk tungsten divertor row in JET (red coloured for indication); each block contains 24 lamellae stacked with sandwiched spacers for an appropriate castellation pattern.

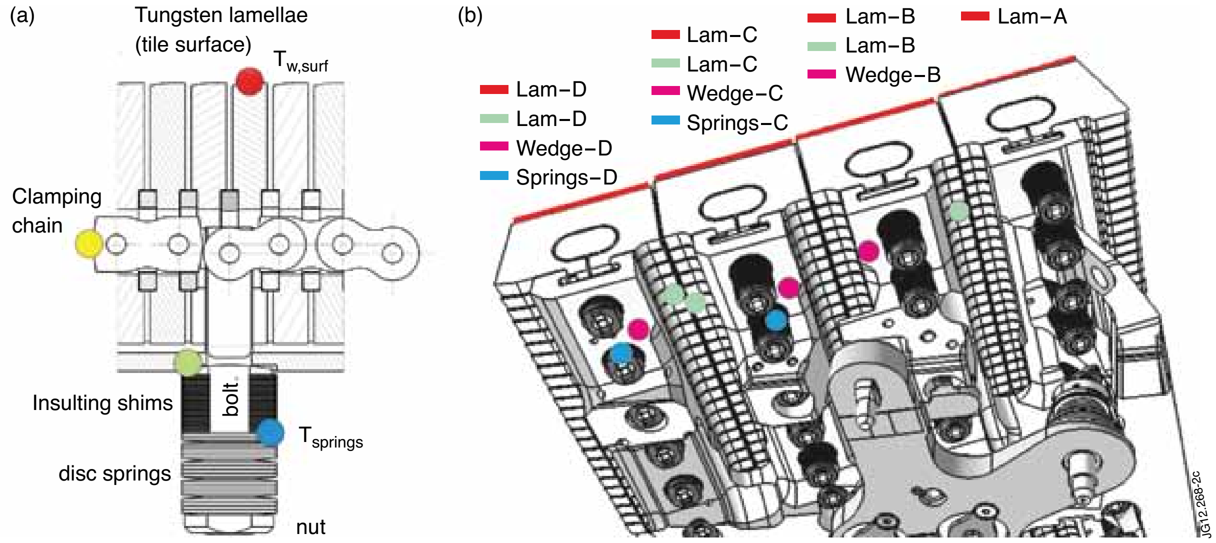

Figure 2: (a) Left: position of the main thermocouples in the most recent prototype exposed in MARION (picture from [4]); the green dot is on the clamping rail. (b) Right: corresponding positions in dedicated assemblies in JET: no TC on the clamping chain, the temperature at the bottom of the carrier is indicated in purple. Some of the TCs are redundant (distributed over a couple of assemblies). In both cases, the red TW,surf   is an infrared measurement.

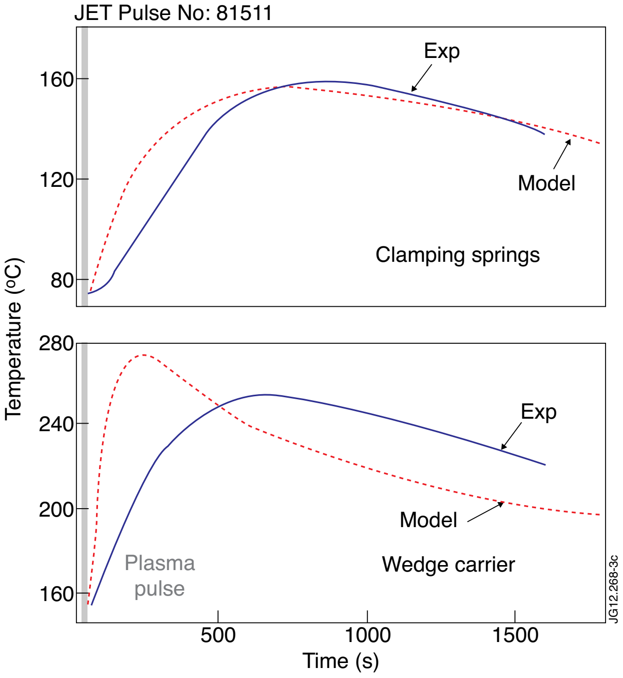

Figure 3: Measured (solid line) and expected (GTM model, dashed line) temperature curves versus time for the clamping spring discs (top) and for the wedge carrier (bottom).